

# EVLA Memo 121

## EVLA L-, K-, and Q-Band Focus Analysis

Brigette Hesman, Rick Perley and Ken Sowsinski  
NRAO

February 11, 2008

### Abstract

The variation of subreflector position with frequency was measured at L-, K-, and Q-band. As expected, the L-band focus relation is non-linear between the band edges while the K- and Q-band relations are linear. The focus position at L-band varies by  $\sim 3$  cm and by  $\sim 1$  mm at both K- and Q-band. This analysis indicates that setting the focus position for a frequency at the center of each band has at most a 1% effect on efficiency when observing at the edges of the band.

## 1 Introduction

In EVLA Memo 109 (Figure 9), the efficiency of antenna 14A was measured as a function of subreflector position for frequencies from 1100 to 2000 MHz. The results showed that the highest efficiency occurred at different focus positions depending on the frequency being observed. Currently, all observations are performed using a focus position measured at the standard frequency in each band for each antenna. An analysis of the focus relation with frequency at L-, K-, and Q-band was performed to determine the effect this practice has on efficiency and determine the focus relation with frequency in each band. The initial focus positions,  $z_{in}$ , for L-, K-, and Q-band for the EVLA antennas are given in Table 1.

The variation of amplitude as a function of the focus offset and frequency, for each antenna, was measured while observing a calibrator. The results of these observations are presented below.

## 2 Observations

All observations were done in continuum; 25 MHz at L-band and 50 MHz at K- and Q-band. The subreflector was moved to seven measurement positions in increments of 2 cm at L-band; while the K- and Q-band increments were determined by scaling the L-band value by a ratio of the wavelengths. The focus curves at each frequency were measured by adjusting the position of the subreflector using escaper commands within the VLA observe file. An example of an escaper which offsets the initial subreflector position by 6 cm is as follows:

```
/** \subarray.setFocusOffset(6)
```

The L-band frequencies were chosen to avoid known RFI. In K- and Q-bands, reference pointing was performed before the focus measurements proceeded. Table 2 summarizes the observations in each band.

Antenna Number	L-Band $z_{in}$ (cm)	K-Band $z_{in}$ (cm)	Q-Band $z_{in}$ (cm)
1	-1.0	2.5	n/a
11	-2.5	2.8	2.9
13	-4.0	2.0	2.4
14	-6.0	0.75	0.75
16	-9.0	-1.9	-1.8
17	-1.5	2.8	3.0
18	-3.0	2.6	2.7
19	-5.0	0.0	0.0
21	0.0	4.7	5.0
23	0.0	4.9	5.2
24	-5.0	0.1	0.6
25	-3.0	2.3	2.3
26	-7.0	-1.0	-0.4

Table 1: The initial focus positions for L-, K-, and Q-band for the EVLA antennas (measurements done by Ken Sowinski).

Band	Source	Bandwidth	Frequencies Observed	Subreflector Position Increment (cm)
L	0542+498	25 MHz	1185, 1235, 1315, 1435, 1515, 1665, 1765, 1865, 1985, 2035 MHz	2
K	0319+415	50 MHz	18, 19, 20, 21, 22, 23, 24 25, 26, 26 GHz	$2 * (\frac{\lambda_K}{\lambda_L}) = 0.13$
Q	0319+415	50 MHz	39, 40, 41, 42, 43, 44, 45, 46, 47, 48, 49, 50 GHz	$2 * (\frac{\lambda_Q}{\lambda_L}) = 0.06$

Table 2: Summary of the observations.

### 3 Analysis

The data were loaded into AIPS as correlation coefficients and reduced using the standard method. After running the AIPS task *calib* the data were read into IDL and the amplitude gain coefficients,  $A$ , versus focus offset,  $z$ , were fit to a quadratic curve of the form,

$$A(z) = A_{min}(1 + a(z - z_o)^2), \quad (1)$$

where  $A_{min}$  is the normalization amplitude and  $a$  is a measure of the curvature of the quadratic. Since the nominal focus position can vary with frequency,  $z_o$  is a measure of the offset of the initial value,  $z_{in}$  (values listed in Table 1), from the true focus value,  $z_{true}$ . As examples, Figures 1 to 3 show the normalized amplitude gain coefficient data points ( $A/A_{min}$ ) versus focus offset and the fit of Equation 1 for antenna 26 at sample frequencies in L-, K-, and Q-band.

Using the results of fitting Equation 1 to the gain curves for each antenna and frequency the true focus position,  $z_{true}$ , was calculated by adding the initial focus values,  $z_{in}$  listed in Table 1, to the derived focus offset value,  $z_o$ ,

$$z_{true} = z_o + z_{in}. \quad (2)$$

This produced a relation of focus position with frequency in each band for each antenna. Many antenna had spurious results at this stage because of amplitude gain curves that did not exhibit a

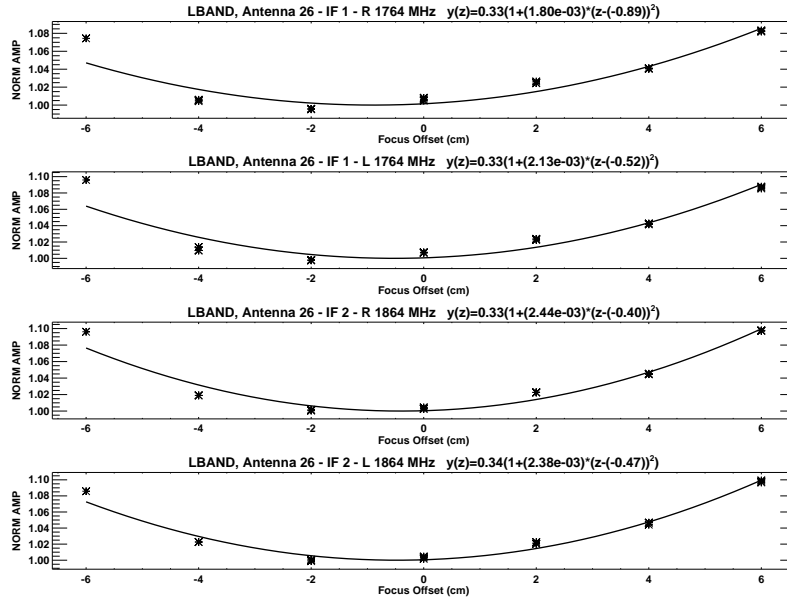


Figure 1: Best-fit quadratic focus curves to the L-band measurements at frequencies 1764 and 1864 MHz for both polarizations. EVLA antenna 26.

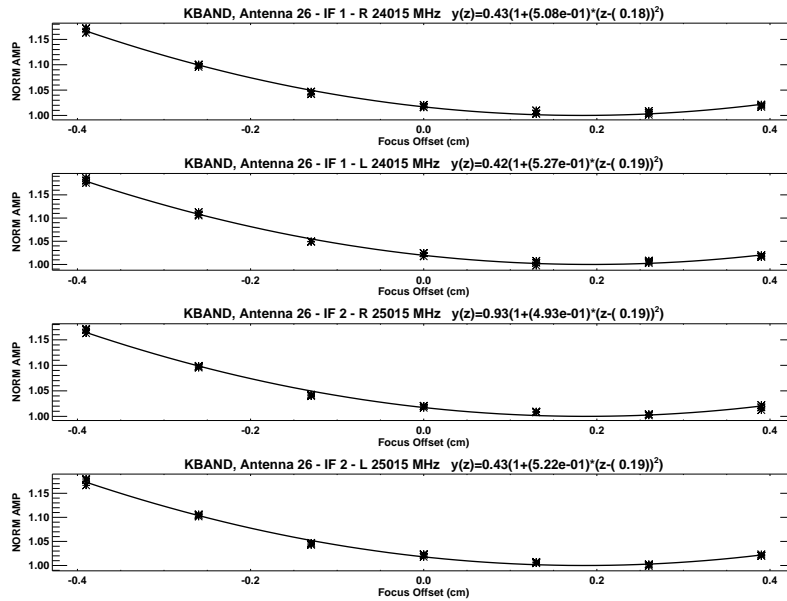


Figure 2: Best-fit quadratic focus curves to the K-band measurements at frequencies 24 and 25 GHz for both polarizations. EVLA antenna 26.

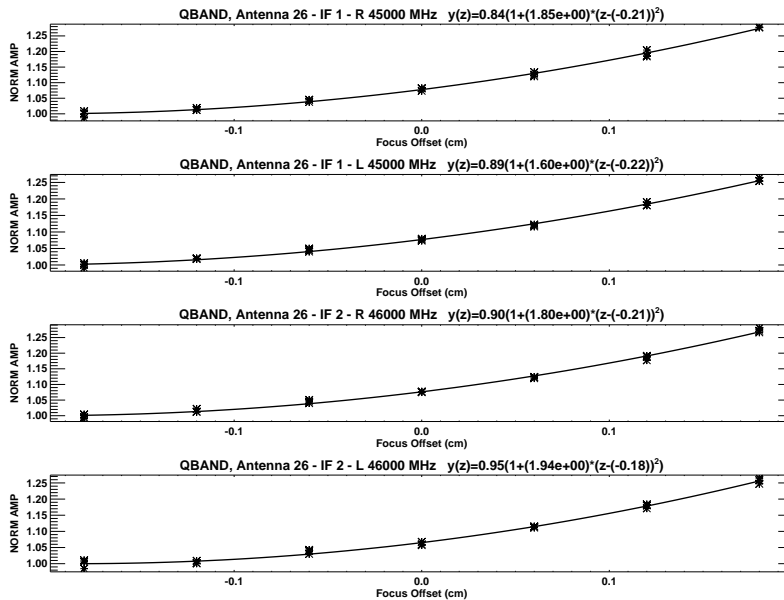


Figure 3: Best-fit quadratic focus curves to the Q-band measurements at frequencies 45 and 46 GHz for both polarizations. EVLA antenna 26.

step relation with subreflector position. These antenna likely suffered from incomplete subreflector movement due to problems with the focus rotation mount. Therefore, any antenna that did not show the expected step curve behavior was eliminated. The focus relation for each antenna was normalized to produce a general focus relation in each band. This was accomplished by subtracting the median focus position,  $z_m$ , for each antenna from the true focus position,

$$z_c = z_{true} - z_m. \quad (3)$$

At each frequency, the median subtracted focus positions for each antenna,  $z_c$ , were averaged to produce a single value,  $\bar{z}_c$ , with the uncertainty in that value,  $\sigma_{\bar{z}_c}$ , defined as the standard deviation in the mean,

$$\bar{z}_c = \frac{\sum_{i=1}^N z_{c_i}}{N}, \quad (4)$$

$$\sigma_{\bar{z}_c} = \frac{\sigma_{z_c}}{\sqrt{N}}, \quad (5)$$

where  $N$  is the number of EVLA antennas included in the calculation. Curve fitting was then applied to determine the relation of focus position with frequency in each band. Figures 4-6 show the results of these calculations and Table 3 presents the focus relations for each band.

## 4 Results

We find that the focus position at Q-, K-, and L-band does vary with frequency; at L-band the relationship is non-linear which was also shown in the total power measurements in Figure 9 of EVLA Memo 109. The expected result, from the L-band feed horn design (EVLA Memo 87), is shown as the dashed curve in Figure 4 and is a reasonable comparison to the best-fit quadratic curve to the L-band measurements. The dashed curve was derived using measurements across L-band of the phase center distance from the aperture plane (Table 1; EVLA Memo 87). As the phase center

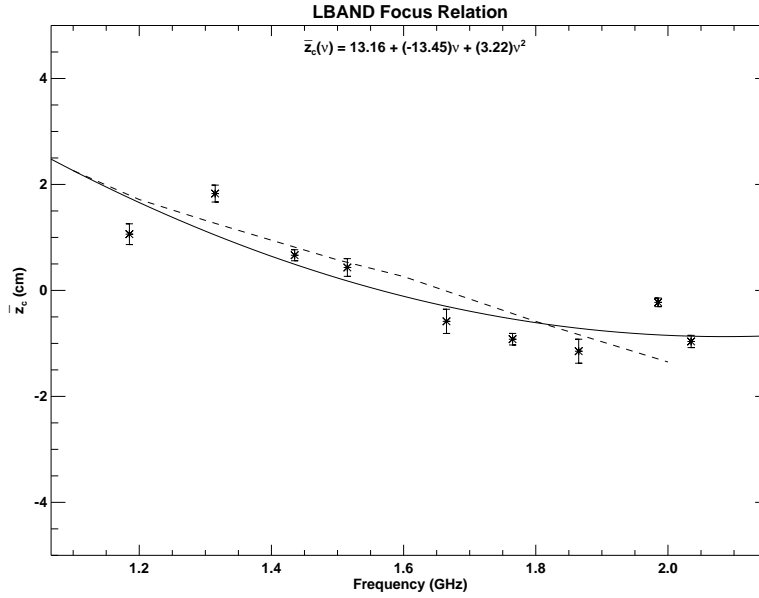


Figure 4: L-band focus relation. The data points are the antenna averaged values for each frequency. The solid line is the best-fit relation to the data points. The dashed curve is the expected result based on measurements of the phase center distance from the aperture plane of the L-band feed horn.

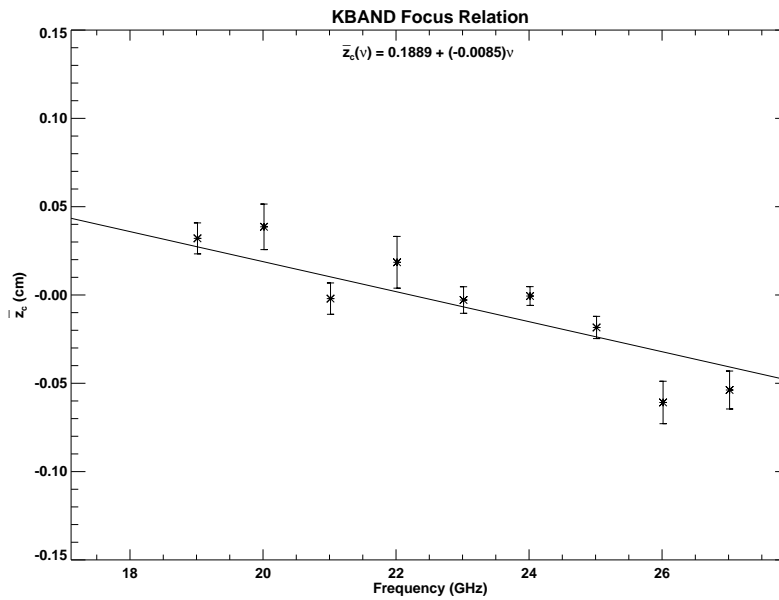


Figure 5: K-band focus relation. The data points are the antenna averaged values for each frequency. The solid line is the best-fit relation to the data points.

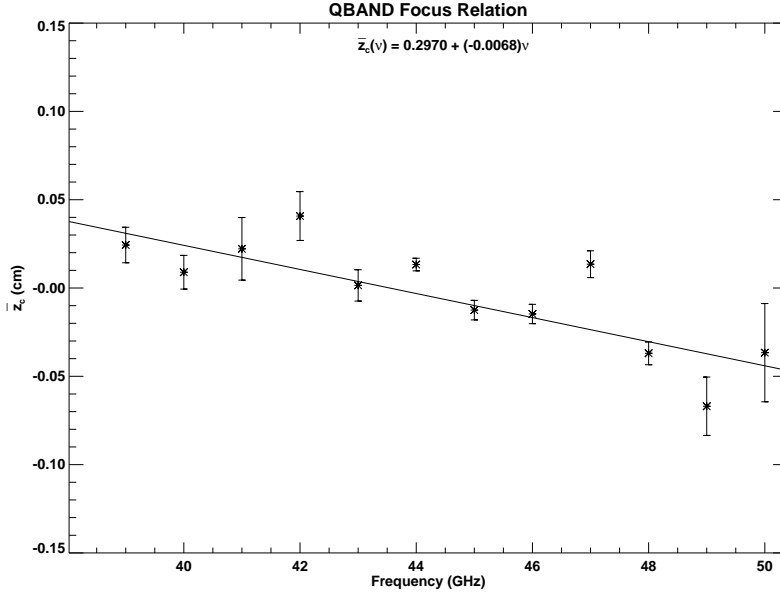


Figure 6: Q-band focus relation. The data points are the antenna averaged values for each frequency. The solid line is the best-fit relation to the data points.

Band	Median $a$	Focus Relation
L	0.0016	$\bar{z}_c(\nu) = 13.16 - 13.45\nu + 3.22\nu^2$
K	0.4	$\bar{z}_c(\nu) = 0.1889 - 0.0085\nu$
Q	1.7	$\bar{z}_c(\nu) = 0.2970 - 0.0068\nu$

Table 3: L-, K-, and Q-band median values of the curvature (central-band values),  $a$ , and the focus relations; where  $\bar{z}_c$  is the focus position in cm and  $\nu$  is the frequency in GHz. The curvature values at the edge of the bands can be derived from scaling the central-band values listed by a ratio of the square of the frequencies.

position  $d_{\phi_c}$  increases with increasing frequency the change in subreflector position between two frequencies,  $\Delta\bar{z}_c$ , can be estimated using,

$$\Delta\bar{z}_c = \frac{\Delta d_{\phi_c}}{M^2}, \quad (6)$$

where  $\Delta d_{\phi_c}$  is the change in the position of the phase center between two frequencies and  $M$  is the magnification. The change in subreflector position,  $\Delta\bar{z}_c$ , was converted to subreflector position,  $\bar{z}_c$ , using,

$$\bar{z}_c = \bar{z}_c(@1.1 \text{ GHz}) + \Delta\bar{z}_c, \quad (7)$$

where  $\bar{z}_c(@1.1 \text{ GHz})$  is the focus position at 1.1 GHz. The dashed curve is therefore not an absolute measurement but rather determined relative to a low-frequency focus position. The K- and Q-band horns however have linear tapers and the phase center position is almost constant with frequency. Because of this, there is expected to be a very small change in focus position with frequency which is demonstrated in Figures 5 and 6.

The focus relations for L-, K-, and Q-band are used to estimate the efficiency loss when observing at the edges of the band using a focus position set by a central band frequency. Figure 9 of EVLA Memo 109 showed that the optimum focus position varied by about 4 cm across L-band. The loss

of efficiency, at all frequencies, was found to be less than 2% by setting the focus position to the median value (-5 cm). This analysis shows that the variation in focus position is  $\sim 3$  cm at L-band and  $\sim 1$  mm at both K- and Q-band. The amplitude gain coefficients,  $A$ , output by *calib* are a direct measure of efficiency,  $\epsilon$ ,

$$A = \frac{1}{6.1} \sqrt{\frac{T_{sys}}{\epsilon}} \quad (8)$$

where  $T_{sys}$  is the system temperature (Equation 6; EVLA Memo 119). If the focus position is set using a frequency at the center of the band it is possible to determine the effect this will have on efficiency when observing at the edges of the band. The amplitude gains at the edges and center of the band are estimated using Equation 1 and the median values for  $a$  and focus relations listed in Table 3. Using these derived amplitude gains and applying Equation 6 allows the efficiency at the edges of the band to be related to the central band efficiency through,

$$\epsilon_{be} = \left( \frac{A_{bc}}{A_{be}} \right)^2 \epsilon_{bc}, \quad (9)$$

where  $\epsilon_{be}$  is the efficiency at the edge of the band,  $A_{bc}$  and  $A_{be}$  are respectively the amplitude gains at the center and edge of the band when the focus position is set using a frequency at the center of the band, and  $\epsilon_{bc}$  is the efficiency at the band center. These focus relations indicate that the efficiency loss at the edges of the band will be less than 1% and 0.5% at L- and K-band respectively and approximately 1% at Q-band.

## 5 Conclusions

The above analysis indicates that the focus relations across L-, K-, and Q- bands are as expected; non-linear (quadratic) for L-band and linear for K- and Q-band. The non-linear structure of the L-band relation was an expected result due to the feed design (see EVLA Memo 85). At lower frequencies in L-band, the focal point accelerates its position upward but as the focus curve also broadens at lower frequencies the quadratic structure of the focus relation at L-band has little effect on efficiency. Therefore, the loss in efficiency by setting the focus position using a frequency at the center of each of the bands is at most 1%.

## 6 Acknowledgement

We would like to thank S. Srikanth for helpful discussion about the L-, K-, and Q-band horn designs and the expected relations that would result from this type of analysis.

## 7 References

- R. Perley and B. Hayward. Wide-Band Sensitivity and Frequency Coverage of the EVLA and VLA L-Band Receivers. *EVLA Memo 119*, 2008.
- R. Perley and B. Hayward. Wideband Performance of the EVLA L-Band System. *EVLA Memo 109*, 2007.
- R. Perley, B. Hayward, and D. Mertely. Testing the EVLA L-Band Feed. *EVLA Memo 85*, 2004.
- S. Srikanth, J. Ruff, and E. Szpindor. Design, Prototyping and Measurement of EVLA L-Band Feed Horn. *EVLA Memo 87*, 2005.